Fayoum University Faculty of Engineering, 2024, Vol: 7(3), 128-143
https://fuje.journals.ekb.eg/
ISSN Online: 2537-0634
ISSN Print: 2537-0626

Electrochemical Evaluation of Biomedical Titanium and Its Alloys in Simulated Body Fluids with Inflammation Condition H_2O_2

Shefaa S. Ali, Mohamed M. El-Rabeie, Nadia H. Helal, Ghada M. Abd El-Hafez and Zeinab R. Farag*

Faculty of Science, Chemistry Department, Fayoum University, 63514 Fayoum, Egypt

*Corresponding author: Zeinab R. Farag (zrf00@fayoum.edu.eg)

How to cite this paper: Ali, S.S., El-Rabeie, M.M., Helal, N.H.. Abd El-Hafez, G.M. & Farag, Z.R. (2024). Electrochemical Evaluation of Biomedical Titanium and Its Alloys in Simulated Body Fluids with Inflammation Condition H_2O_2. *Fayoum University Journal of Engineering*, *Vol: 7(3), 128-143*
https://dx.doi.org/10.21608/FUJE.2024.231975.1059

Abstract

Titanium and Ti-alloys are recognized as corrosion resistant alloys, which have biomedical applications as orthopedic implantations due to this film of titanium oxide formed on its surface. However, the inflammatory conditions could affect the corrosion resistance of this alloy. The research work aims to investigate the electrochemical behavior of commercial virgin titanium and aspects of blending it with either V or Al on its resistivity. The study was extended to include the effect of addition of H_2O_2 on the corrosion behavior of Ti and Ti-alloys. The electrochemical behavior of the pure Ti and its alloys Ti-4AL-2V and Ti-6Al-4V was evaluated using the potentiodynamic polarization as well as by electrochemical impedance spectroscopy, EIS. Scanning electron microscope, SEM was used to study the surface morphology of the investigated Ti-alloys. Energy dispersive X-ray analysis, EDX, technique was used to determine the composition of the deposited oxide layer formed on the surface after immersion in the electrolytic solution. On the other hand, the metals released into the electrolyte was detected using atomic absorption spectrophotometry, AAS. It was found that Ti-alloys corrosion resistance was affected by the inflammatory conditions, where the pure Ti has the highest polarization resistance and the smallest corrosion rate when compared with Ti-4AL-2V and Ti-6Al-4V alloys.

Keywords

Corrosion behavior, Potentiodynamic Polarization, EIS, Ti alloys, Simulated Body Fluids, Biomedical

1. Introduction

Biomedical materials are commonly used in the replacement and repair of human tissues, and it requires a multidisciplinary approach to ensure that these materials implanted in living organisms do not cause adverse reactions. After being inserted into the body, the materials may rub against human tissue or other implants, causing the implants to deteriorate over time. Osteolysis and

inflammation may bring on by the wear and tears of implants in the human body can have an impact on both the health of the patient and the longevity of the implant [1, 2]. Surgical procedures are used to repair, replace, or regenerate damaged tissue [3]. Alternative biomaterials was developed to avoid the problems caused bio-implants such as Ni-toxicity, corrosion degradation and others [4, 5].Titanium and its alloys are one of the widely used components that have biomedical applications [6-9] due to their higher corrosion resistance, good biocompatibility and they also have special features including high specific strength and osseointegration as well [10, 11] . In addition, Ti, and Ti-alloys can be used to replace hard tissues in orthopedics [12-15]. The higher passivation of Ti and Ti-alloys was attributed to the formation of a spontaneously, passive and thermodynamically stable TiO_2 protective layer [15, 16]. Alloying Ti with different metals may be resulted in modulation of the alloy properties, such as hardening and tensile strength [17, 18]. Although their excellent mechanical properties and non-cytotoxicity Ti and Ti alloys have some disadvantages such as their biological inertness and poor antibacterial properties, which inhibits their further development.

Various studies on the corrosion behavior of Ti and Ti-alloys have been reported [17, 19-24], and investigated in different media [25, 26]. There are various parameters, which may significantly affect the corrosion behavior of Ti-alloys such as corrosion medium, pH and temperature [27]. In addition, the physiological species in simulated physiological environments may also influence the corrosion behavior [28-35]. The effect of proteins and reactive oxygen species on the corrosion behavior of Ti-6Al-4V was reported [36]. It was noticed that the activities of Reactive Oxygen Species (ROS) ROS can cause serious pathological disorders such as diabetes, ageing and neurodegradation when they overwhelm the body's antioxidant mechanisms [37]. Hydrogen peroxide (H_2O_2) is an important oxidizing component and a factor that may influence the corrosion process of Ti-alloys [38]. Enzymes in the body destroy superoxides by catalyzing their conversion to hydrogen peroxide (H_2O_2), which potentially damaging the implanted materials [39, 40]. In the present work aims to investigate the effect of aggressive simulated inflammatory conditions on the electrochemical properties of Ti and its alloys. In order to simulate the per implant inflammatory conditions *in-vitro* studies were conducted with addition of H_2O_2. Different electrochemical techniques, e.g. polarization techniques and EIS, were used essential to clarify the fundamentals of the corrosion / passivation processes, which may occurs at the alloy solution interface. The morphology of the alloy surface was analyzed by EDX and SEM.

2. Experimental procedures

2.1. Electrochemical cell

An experimental method was developed to investigate the corrosion behavior of Ti and Ti-alloys in simulated body fluids and in H_2O_2 as an inflammation medium. Samples of Ti and some of its alloys with different Al, V content (Ti-4Al-2V and Ti-6Al-4V) were used. The Ti-samples were obtained from different sources such as plates and screws then they were fabricated into rods to fit the measurement cell. The chemical compositions of prepared alloys are listed in Table 1.

The electrochemical cell with three electrodes working electrode (Ti alloys surface area was 0.283, 0.196 and 0.196 cm^2 for Ti, Ti-4Al-2V and Ti-6Al-4V respectively), the counter electrode was a Pt-electrode and a saturated calomel electrode (SCE) as a reference electrode. Before experimental work, the alloy surface was polished using emery papers up to 3000 grit, rubbed and then extensively washed with deionized water.

2.2. Solutions

The chemical composition of the electrolyte solutions, which simulate the physiological conditions of the human body with pH 7.5 were used for *in vitro* corrosion studies was given in Table 2 [41]. As reported in the literature, a volume of 50 mM H_2O_2 solution titrated to pH 5.0 was used to simulate inflammatory conditions [42].

2.3. Techniques

I. A digital pH meter was used to adjust the pH during tests. The electrochemical measurements were performed using 150 mL solution at 37 °C ± 0.2 °C and for reproducibility, each experiment was repeated three times.

II. The electrochemical measurements were performed on the Voltalab 10 PGZ100 "All-in-one "potentiostat/ Galvanostat. Open circuit potential (OCP) was used to record the EIS experiments, which was monitored for 120 h under simulated body fluid and in inflammation conditions [41, 43]. The potentiodynamic measurements were conducted at a scan rate of 10 mV/s.

III. The concentration of released metals was measured using atomic absorption spectroscopy (AAS) using a SHIMADZU AA7000 analyst instrument with ASC-7000 auto-sampler and GFA-7000 graphite furnace atomizer.

IV. The surface morphology and elemental composition of the tested alloys were investigated before and immersion in the simulated inflammation for 120h using scanning electron microscopy (SEM) of type ZEISS Gemini SEM-field emission scanning electron microscope with an X-ray diffraction patterns (EDX) were collected using Cu-Ka monochromatic radiation at room temperature on a Bruker D8 ADVANCE diffractometer.

3. Results and Discussion

3.1 Electrochemical Measurements

3.1.1 Potentiodynamic Polarization Measurement

Corrosion behavior of Ti-alloys was determined by estimating the chemical composition of alloys, dissolved elements, formation of titanium oxide (TiO_2) and by catalyzed decomposition of the peroxide [44]. Linear polarization was used to evaluate the corrosion behavior of pure Ti and Ti-alloys in simulated body fluids either in absence or in the presence of H_2O_2. The more negative shift of the potential, the lower i_{corr} and the higher corrosion passivation, which in turn led to decreasing in the corrosion rate [45].

Figure 1(a, b) showed the potentiodynamic polarization curves of the pure Ti , Ti-4Al-2V and Ti-6Al-4V samples in simulated body fluid (SBF) and under simulated inflammation condition after immersion for 120 h. It was found that the corrosion current density decreased for Ti-4Al-2V and Ti-6Al-4V samples, which were tested in SBF compared to the samples, which are tested in inflammation condition (SBF/H_2O_2), this is may be attributed to the formation of a protective passive film on the alloy surface.

Over immersion at different times is represented in Figures (2, 3), the i_{corr} was significantly higher for Ti than other alloys in SBF and for Ti-4Al-2V in SBF/ H_2O_2. In SBF, the presence of Al, V in the tested samples increased the stability of the deposited passive film, where V act as a β-stabilizing element while Al is an α-stabilizing element, while in SBF/H_2O_2 the charge transfer resistance CpTi of the formed oxide on Ti-surface was extremely high if compared to that's of Ti-6Al-4V and Ti-4Al-2V. So, the smaller slope of CpTi was due to the increased charge transfer kinetics across its oxide film [41].

The polarization parameters after different immersion times were calculated from the polarization curves, and their values are represented in Tables (3-8). The corrosion rate values of pure Ti, Ti-4Al-2V and Ti-6Al-4V alloys after immersion for different times in simulated body fluid with and without H_2O_2 were calculated from the equation:

$$Corrosion\ rate\ (mm/y) = 3.27 \times 10^{-3} \times icorr(\mu A/cm^2) \times M(g/mol)/[n \times d(g/cm^3)] \quad (1)$$

The results of the variation of the corrosion rate with the immersion time showed that the corrosion rate decreased with increasing of the immersion time. The anodic polarization film became more stable as a result of the dissolution of the metal and formation of a passivated film.

3.1.2. Electrochemical impedance spectroscopy (EIS)

The open-circuit impedance (OCI) for pure Ti and the

investigated alloys were traced over 120 h after electrode immersion in the simulated body fluid with and without H_2O_2 solutions. The recorded impedance spectra were analyzed as Nyquist plots as shown in Figure (4). Generally Nyquist plots showed an increased R_p values were reported for Ti-4Al-2V and Ti-6Al-4V alloys in SBF/H_2O_2 solution compared to SBF solution. The opposite behavior was observed for pure Ti. The electrochemical impedance for pure Ti and their alloys were investigated with different working time in the SBF medium.

The recorded impedance spectra were analyzed as Nyquist and Bode plots as shown in Figures (5-7). Bode plots (*see* figures 5-7 a) for pure Ti and its alloys in SBF at different immersion time showed two-phase maxima peaks appeared in the phase angle plots. The presence of two-phase maxima at both low and high frequencies in Bode plots for all of the investigated samples indicated that the corrosion process was controlled by two-time constants. The first, at the low-frequency region may be attributed to the charge transfer resistance, R_{ct}, and the double-layer capacitance, C_{dl}, at the electrode surface. At higher frequency, the second time constant was due to the formation of a partially protective film **[46]**. On the hand, Bode plot showed that the total impedance (Z) increased with time, which explained the formation of a progressive passive film until a steady state was obtained **[47-49].** The gradual increase of the phase maximum with the increase of the immersion time revealed a decrease in the corrosion rate [48].

In Nyquist plots, the impedance spectra were nearly the same except for the diameters of the loops assigning the corrosion resistance (see Figures 5, 6 and 7 b), this similarity indicated that the corrosion mechanism of the tested alloys were similar but with different corrosion rates **[50]**.

An equivalent circuit models was suggested to enable an accurate analysis of the EIS data Figure 8 and the calculated equivalent circuit parameters for the different alloys in the SBF solution were presented in Tables (9-11).

Tables (9-11 showed that R_p values increased with increasing immersion time while C_{dl} decreasing. The low capacitances could be associated with both an increase of the thickness of the passive layer and a decrease of the dielectric constant of the oxide film, which are conducive to a nobler electrochemical corrosion behavior. Thus, the corrosion resistance of the biomaterials are better visualization of the effect of the simulated solution.

The steady state impedance, of pure Ti and the investigated alloys were traced over 120 h from electrode immersion in the inflammatory conditions. Nyquist plots for pure Ti and its alloys in SBF/H_2O_2, at different immersion time were presented in Figure (9). The results indicated that the film resistance follows the order Ti-6Al-4V> Ti-4Al-2V >Ti. These results are in a good accordance with the polarization measurement results. Adding H_2O_2 to SBF highly decreased the film resistance value for pure Ti and slightly decreased it for Ti-4AL-2V and Ti-6Al-4V alloys as showed in Nyquist plots (*see* Figure 9) **[42, 51].**

The EIS data (Nyquist plots) were fitted according to the equivalent circuit showed in Figure 8. It clearly revealed the presence of two distinguishable time constants as a result of two different processes.

3.2. Surface analysis

The surface morphology of each sample was investigated using SEM after 12 h immersion in solution. The surface of pure Ti, Ti-4Al-2V and Ti-6Al-4V alloys was subjected to EDX analysis to record the different constituents of the passive film. Fig 10 (a, b and c) represents the SEM- EDX measurements of these alloys. Generally, the three elements, Ti, Al, and V are participating in the passivation after 120 h immersion in the inflammation solution at 37^{o}C. The surface morphology of each one represented the ability of each alloy to resist the metal dissolution and forming a passive film to separate the core metal from the corrosive medium. This study was carried out in a highly aggressive inflammation medium to show the behavior of each alloy and determine the feasibility to be used in the human body. The surface morphology of Ti-6Al-4V and Ti-4Al-2V with aluminum and vanadium content was presented and revealed a large degree of film cracks, which made it more susceptible to a different type of corrosion as pitting corrosion and that appeared in EDX results, which revealed a

high Ti, Al concentration for Ti-6A-4V and Ti-4Al-2V alloys . The pure Titanium showed very low cracks on the surface which may be responsible for less or no pits on the surface. The general behavior of these alloys indicated that Al and V content had high dissolution in the inflammatory conditions so it does not improve the alloy performance against corrosion in simulated inflammation conditions at pH 5 and 37°C.

3.3. Metal released Investigation

The metal ions concentrations in the test solutions SBF and SBF/H_2O_2 after the 120 h immersion were measured (Figure 11). It was noticed that in case of pure Ti, the addition of the H_2O_2 did not significantly affect the amount of Ti ions released into the solution, but it was significantly increased the amount of Ti and V ions released in case of Ti-6Al-4V alloy [41]. As stated previously, V is considered as a β-stabilizing element while Al is an α-stabilizing element. Therefore, an increase in the concentration of the released Ti and V ions was accompanied with a constant concentration of the released Al ions, this may be attributed to selective dissolution process [52].

4. Conclusion

The corrosion behavior of pure Ti, Ti-4Al-2V and Ti-6Al-4V alloys in a SBF and SBF/H_2O_2 at the temperature of 37°C was investigated by potentiodynamic polarization and electrochemical impedance spectroscopy. Simulated physiological body solution with constant amount of H_2O_2 was used to simulate the inflammation condition. The results demonstrated that Al and V content in the two alloys did not modify the properties of the pure Ti. The potentiodynamic polarization results indicated that by increasing time pure Ti, Ti-4Al-2V and Ti-6Al-4V attained the lowest i_{corr}, nobler E_{corr} and smallest corrosion rate, which was due to the formation of a protective oxide film. In addition, the experimental impedance results confirmed that increasing time increased the thickness and the resistance of the deposited passive film.

Conflict of interest: no conflict of interest.
Declarations of interest: none.
Data availability statement: The raw/processed data required to reproduce these findings cannot be shared at this time as the data also forms part of an ongoing study

Table 1.Chemical composition of different samples of Titanium (in wt.%)

Alloys	Al	V	O	C	N	Fe	Ti
Pure Ti	-	–	0.25	0.08	0.03	0.04	Balance
Ti –4Al-2V	4.45	1.82	0.25	0.03	0.03	0.03	Balance
Ti–6Al-4V	5.87	4.02	0.30	0.03	0.03	0.04	Balance

Table 2. Reagents amount for preparing 1000 mL of the SBF in gm [42]

Reagent	**NaCl**	**$NaHCO_3$**	**KCl**	**K_2HPO_4 3H2O**	**$MgCl_2$ H2O**	**HCl 1.0 M**	**$CaCl_2$**	**Na_2SO_4**	**TRIS**	**HCl 1.0 M**
SBF	8.035	0.355	0.255	0.231	0.311	39 mL	0.292	0.072	6.118	0-5 mL

Table 3: Potentiodynamic polarization parameters of Pure Ti after different immersion time in SBF/ H_2O_2 at 37 °C.

Time / h	**Ecorr /mV**	**icorr /µA**	**βa /mV**	**βc /mV**	**Corr. Rate / mm/y**
2	-1489.374	158.640	1278.3	-254.1	4.67
24	-1502.927	137.172	746.4	-268.3	4.22
72	-1417.479	115.257	482.2	-278.2	3.55
120	-1467.691	85.431	421.5	-183.5	2.63

Table 4: Potentiodynamic Polarization parameters of Ti-4Al-2V alloy after different immersion time in SBF/ H_2O_2 at 37 °C.

Time / h	**Ecorr /mV**	**icorr /µA**	**βa /mV**	**βc /mV**	**Corr. Rate / mm/y**
2	-1561.658	261.250	4776.8	-467.4	11.63
24	-1489.00	256.33	1898.8	-376.3	11.41
72	-1360.00	222.508	4348.9	-344.0	9.90
120	-1477.310	175.774	931.5	-231.2	7.74

Table 5: Potentiodynamic polarization parameters of Ti-6Al-4V alloy after different immersion time in SBF/ H_2O_2 at 37 °C.

Time / h	**Ecorr /mV**	**icorr /µA**	**βa /mV**	**βc /mV**	**Corr. Rate / mm/y**
2	-1590.017	244.861	1374.4	-330.2	10.90
24	-1525.803	224.359	1123.6	-407.8	9.98
72	-1661.892	188.594	1338.0	-195.8	8.31
120	-1674.749	160.542	714.9	-200.7	7.14

Table 6: Potentiodynamic polarization parameters of pure Ti after different immersion time in SBF at 37°C.

Time / h	Ecorr /mV	icorr /µA	βa /mV	βc /mV	Corr. Rate / mm/y
2	-1 600.0	328.9	2198.4	-342.6	10.14
24	-1 529.4	252.6	1068.7	-290.3	7.79
72	-1 544.1	230.1	1053.4	-267.5	7.09
120	-1 617.4	212.4	849.0	-292.5	6.55

Table 7: Potentiodynamic polarization parameters of Ti-4Al-2V alloy after different immersion time in SBF at 37°C.

Time / h	Ecorr /mV	icorr /µA	βa /Mv	βc /mV	Corr. Rate / mm/y
2	-1 499.2	293.0	2079.1	-352.8	9.03
24	-1 508.0	231.8	955.1	-288.3	7.14
72	-1 494.6	146.0	467.1	-238.4	6.50
120	-1 587.1	194.4	634.2	-265.9	5.99

Table 8: Potentiodynamic polarization parameters of Ti-6Al-4V alloy after different immersion time in SBF at 37 °C.

Time / h	Ecorr /mV	icorr /µA	βa /mV	βc /mV	Corr. Rate / mm/y
2	-1 604.4	273.6	1386.8	-335.0	8.43
24	-1 450.8	212.8	778.3	-267.1	6.56
72	-1 573.6	140.7	408.9	-188.1	6.26
120	-1 646.9	105.3	342.9	-169.5	4.68

Table 9: Electrochemical impedance measurements of pure Ti after different immersion time in SBF at 37°C.

Time / h	Rs /Ω	Rct /kΩ cm^{-2}	Cdl /µF cm^{-2}	α_1	Rpf /kΩ cm^2	Cpf /µF cm^{-2}	α_2
2	4.727	1.717	3.707	0.99	115.9	13.72	0.999
24	6.331	2.025	1.964	0.99	187.5	8.488	1
48	6.053	2.489	2.557	0.99	278.5	5.713	1
72	1.152	3.659	6.871	0.99	322.5	4.934	1
120	4.349	4.995	7.964	.99	580.0	2.744	1

Table 10: Electrochemical impedance measurements of Ti-4Al-2V alloy after different immersion time in SBF at 37°C.

Time / h	Rs /Ω	Rct /kΩ cm^{-2}	Cdl /µF cm^{-2}	α_1	Rpf /kΩ cm^2	Cpf /µF cm^{-2}	α_2
2	4.726	3.153	2.019	.99	124.6	12.76	.99
24	5.272	3.601	0.883	0.99	297.8	4.275	1
48	5.456	4.599	0.865	0.99	334.3	3.008	0.999
72	3.584	4.616	0.217	0.98	371.0	1.715	1
120	11.92	5. 343	0.941	0.99	475.3	1.339	1

Table 11: Electrochemical impedance measurements of Ti-6Al-4V alloy after different immersion time in SBF at 37 °C.

Time / h	Rs /Ω	Rct /kΩ cm^{-2}	Cdl /µF cm^{-2}	α_1	Rpf /kΩ cm^2	Cpf /µF cm^{-2}	α_2
2	4.972	3.718	60.067	0.98	220.9	7.204	0.999
24	23.87	4.104	6.257	0.99	463.4	2.747	1
48	17.80	4.796	4.180	0.99	737.6	1.726	1
72	21.64	4.657	4.305	0.99	947.8	1.679	1
120	19.20	5.561	7.154	0.96	1000.1	1.431	1

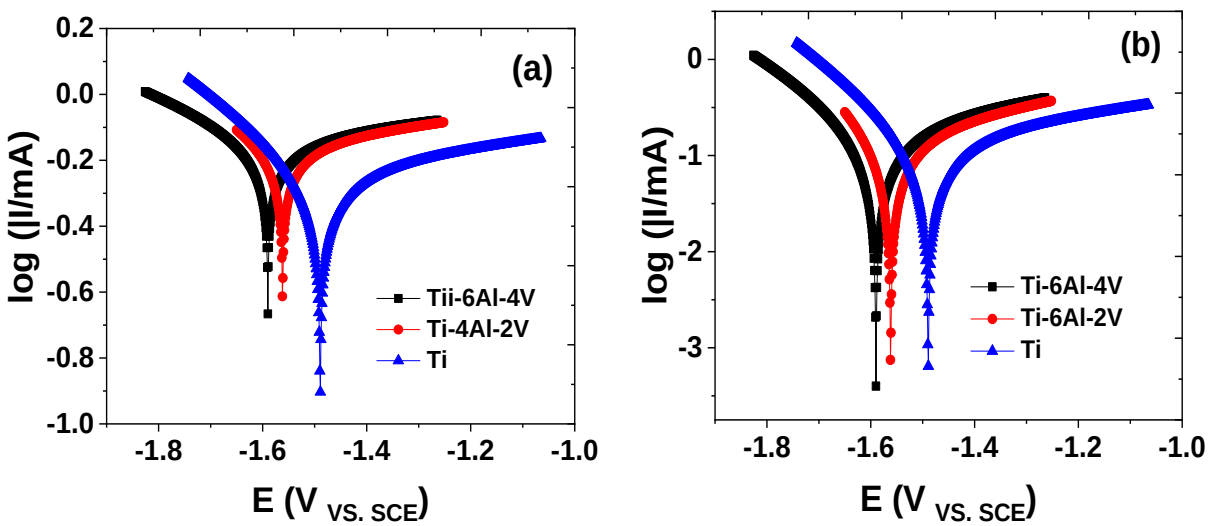

Fig. 1: Potentiodynamic Polarization curves of pure Ti and Ti-4Al-2V and Ti-6Al-4V alloys after 120 h of electrode immersion in (a) SBF (b) SBF/H_2O_2 solutions at 37 °C.

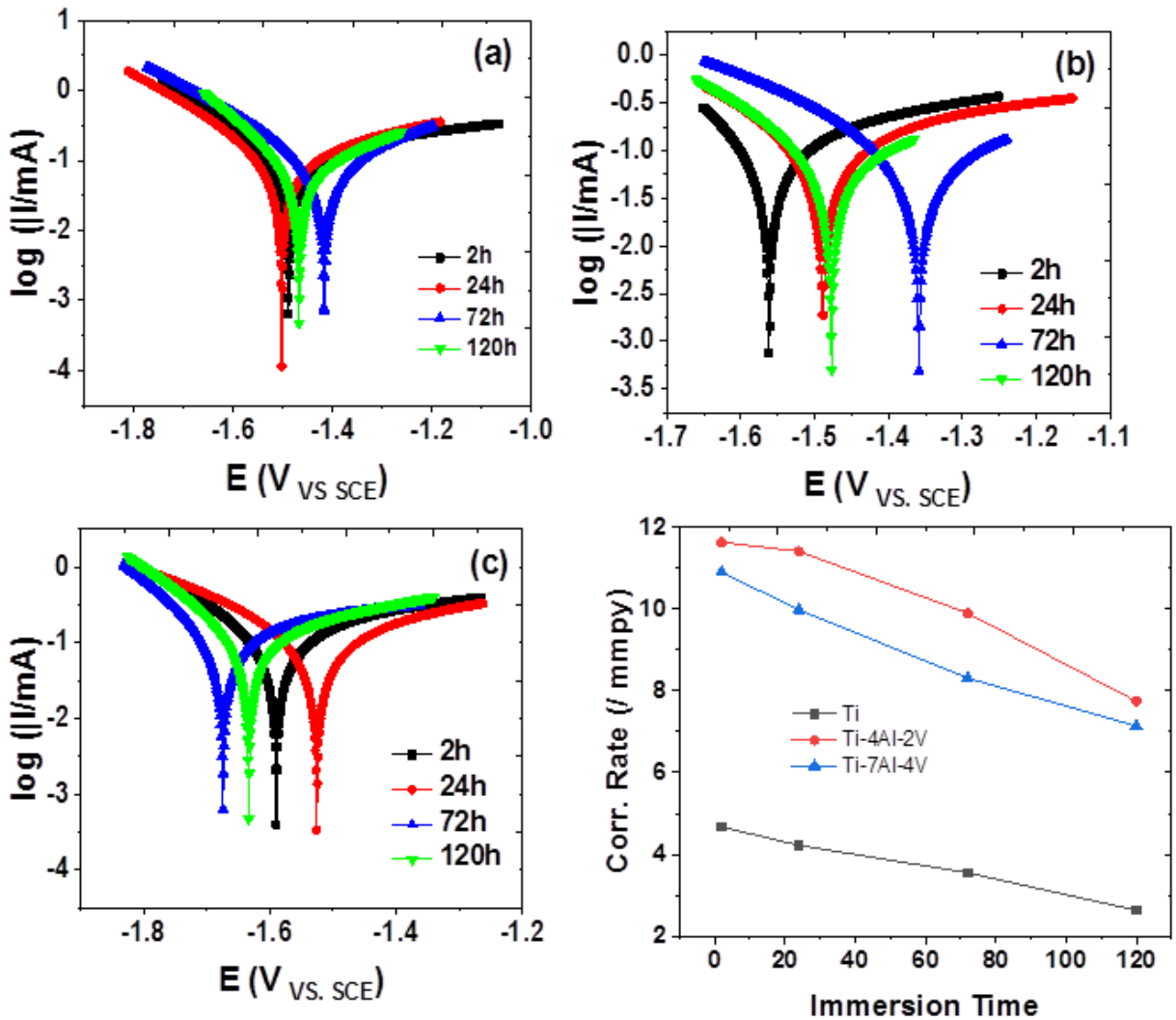

Fig. 2: Polarization curves of pure Ti and Ti-4Al-2V and Ti-6Al-4V alloys in inflammation simulated body fluid with H_2O_2 after different immersion times at 37 °C: (a) pure Ti, (b) Ti-4Al-2V, (c) Ti-6Al-4V and (d) variation of corrosion rate with immersion time.

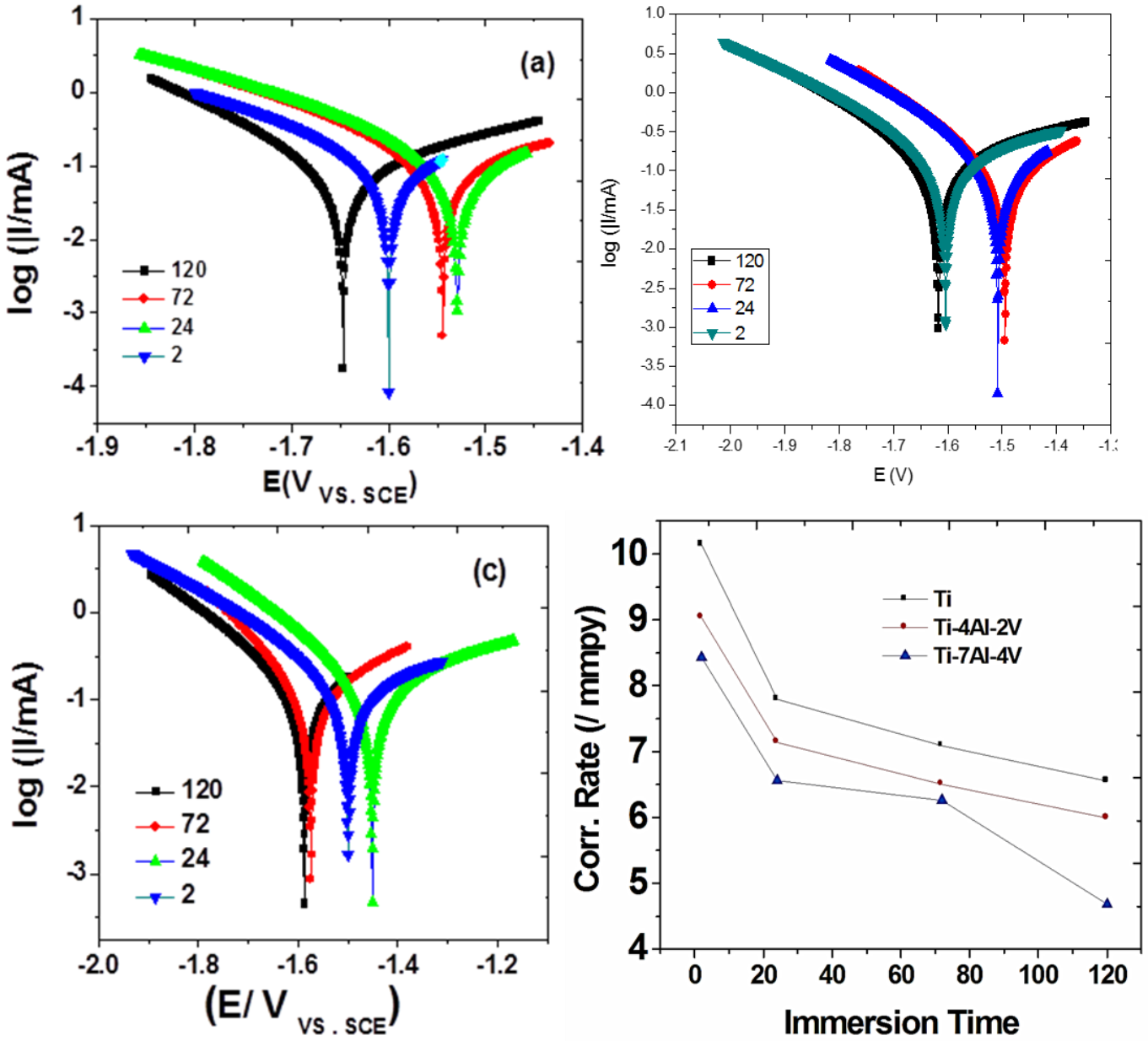

Fig. 3: Polarization curves of pure Ti and Ti-4Al-2V and Ti-6Al-4V alloys in SBF after different immersion times at 37 °C: (a) pure Ti, (b) Ti-4Al-2V, (c) Ti-6Al-4V and (d) variation of corrosion rate with immersion time.

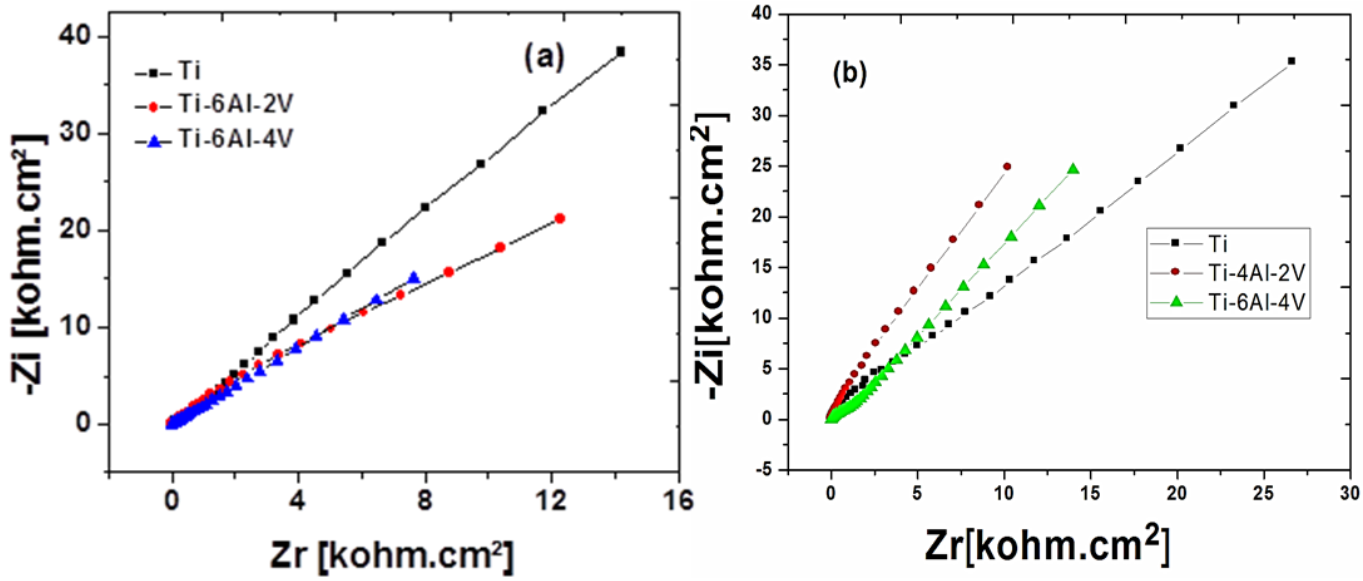

Fig. 4: Nyquist plots for pure Ti, Ti-4Al-2V and Ti-6Al-4V at 120 h from the electrode immersion in (a) SBF (b) SBF/H_2O_2 solutions at 37°C.

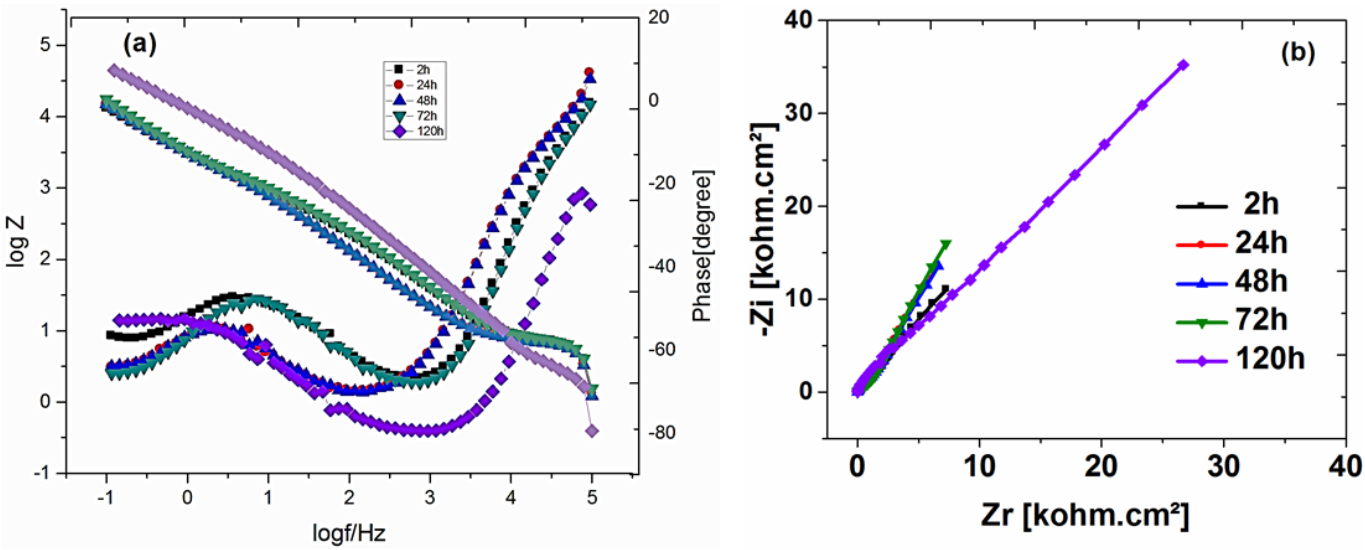

Fig. 5: Nyquist and Bode plots of pure Ti after different immersion time in SBF solution at 37°C.

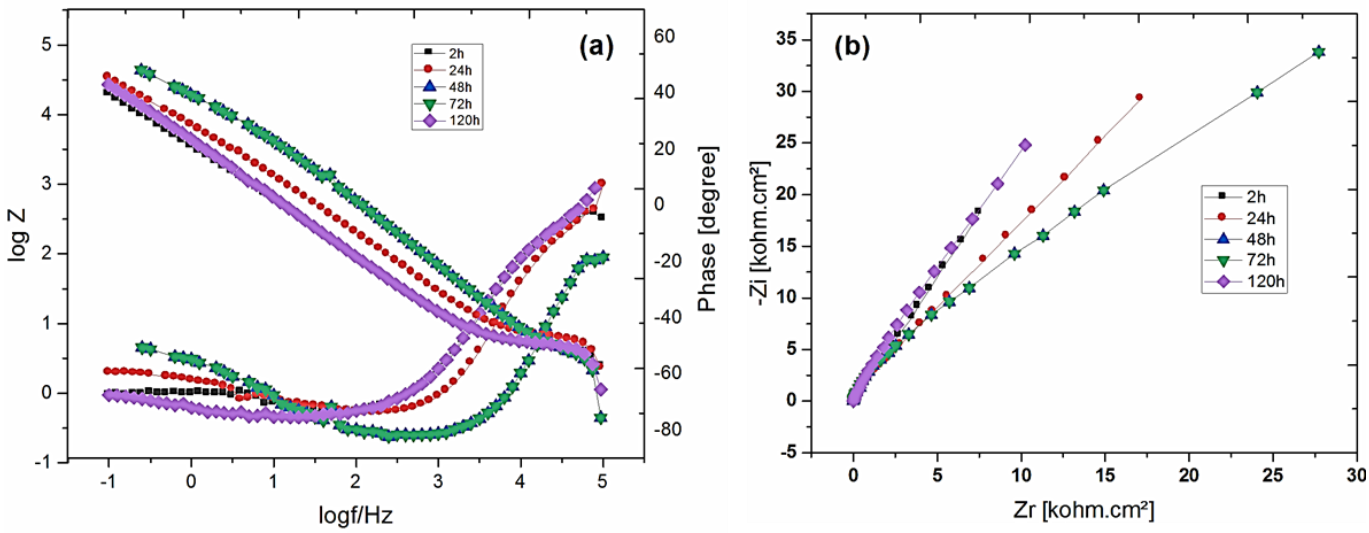

Fig. 6: Nyquist and Bode plots of Ti-4Al-2V alloy after different immersion time in SBF solution at 37°C.

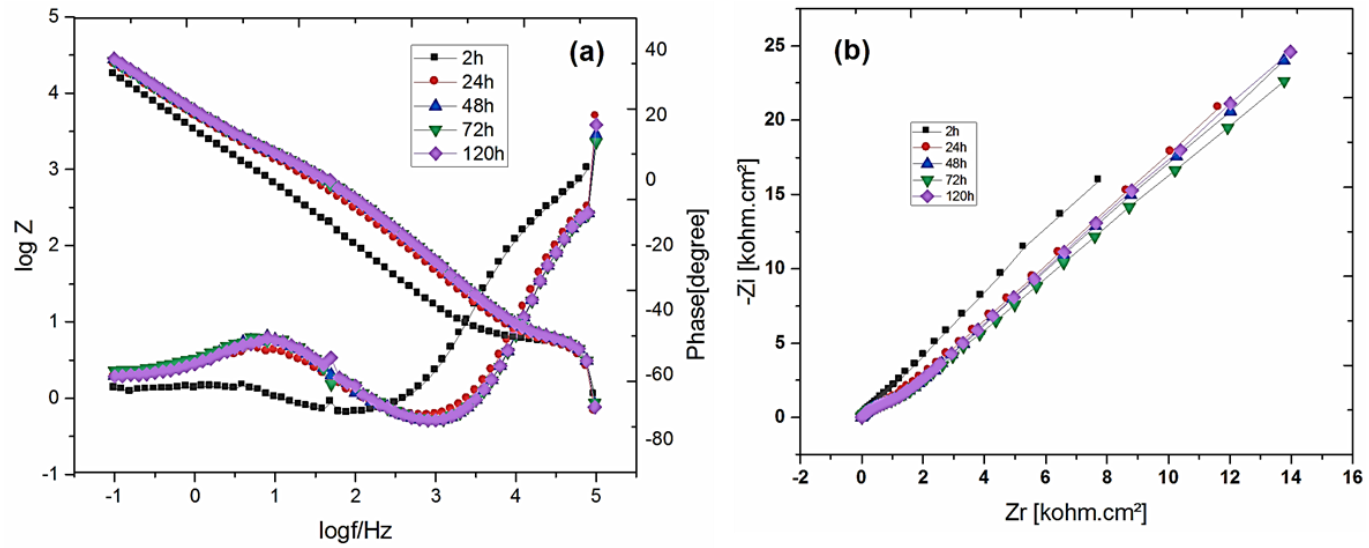

Fig. 7: Nyquist and Bode plots of Ti-6Al-4V alloy after different immersion time in SBF solution at 37°C.

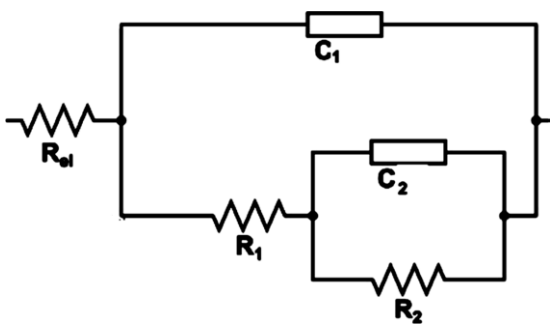

Fig. 8: Equivalent circuit used to model the EIS data recorded on the Ti and its alloys.

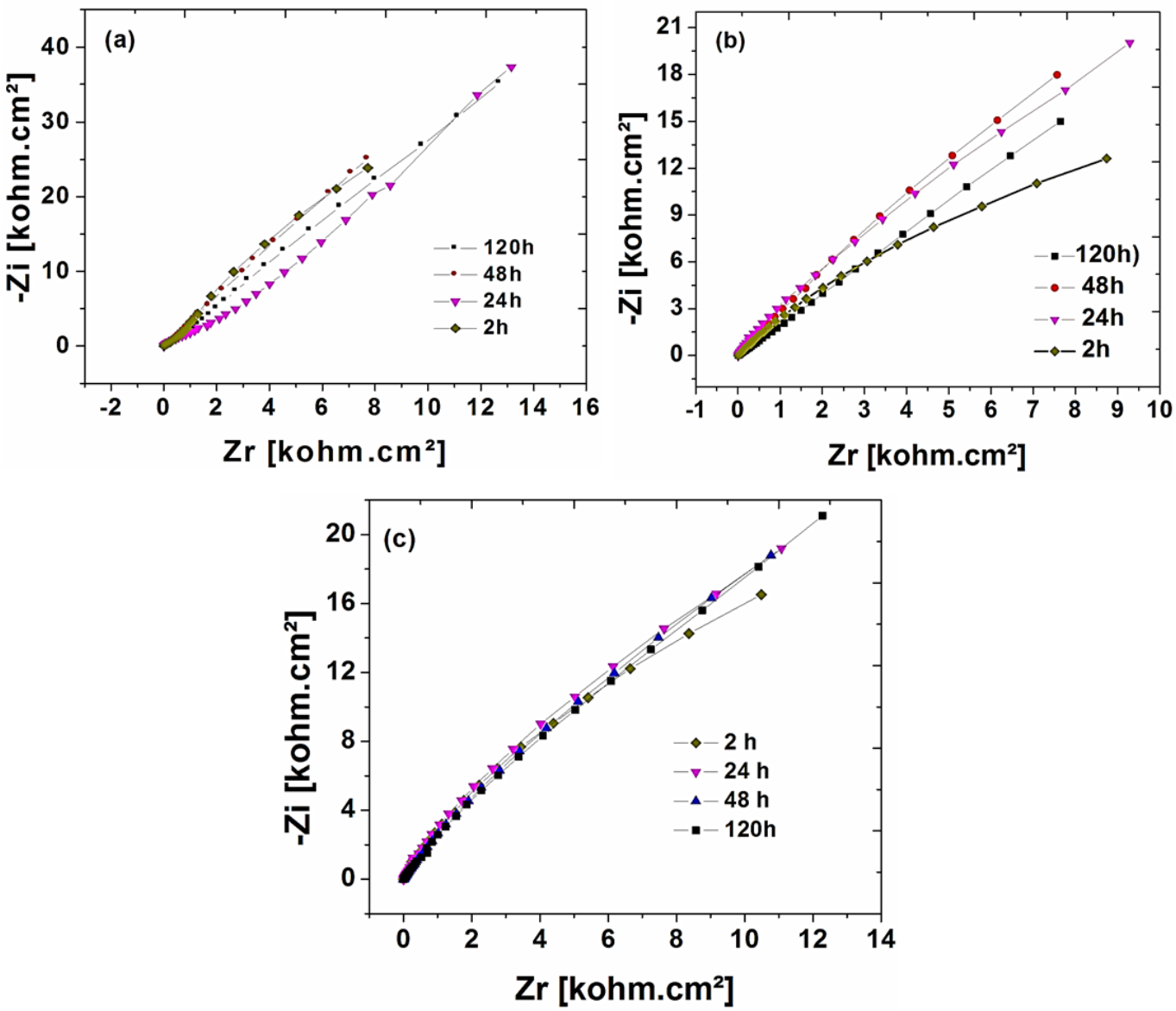

Fig. 9: Nyquist plots for (a) pure Ti, (b) Ti-4Al-2V and (c) Ti-6Al-4V alloys after the immersion of the electrode in SBF /H_2O_2 solution at 37 °C.

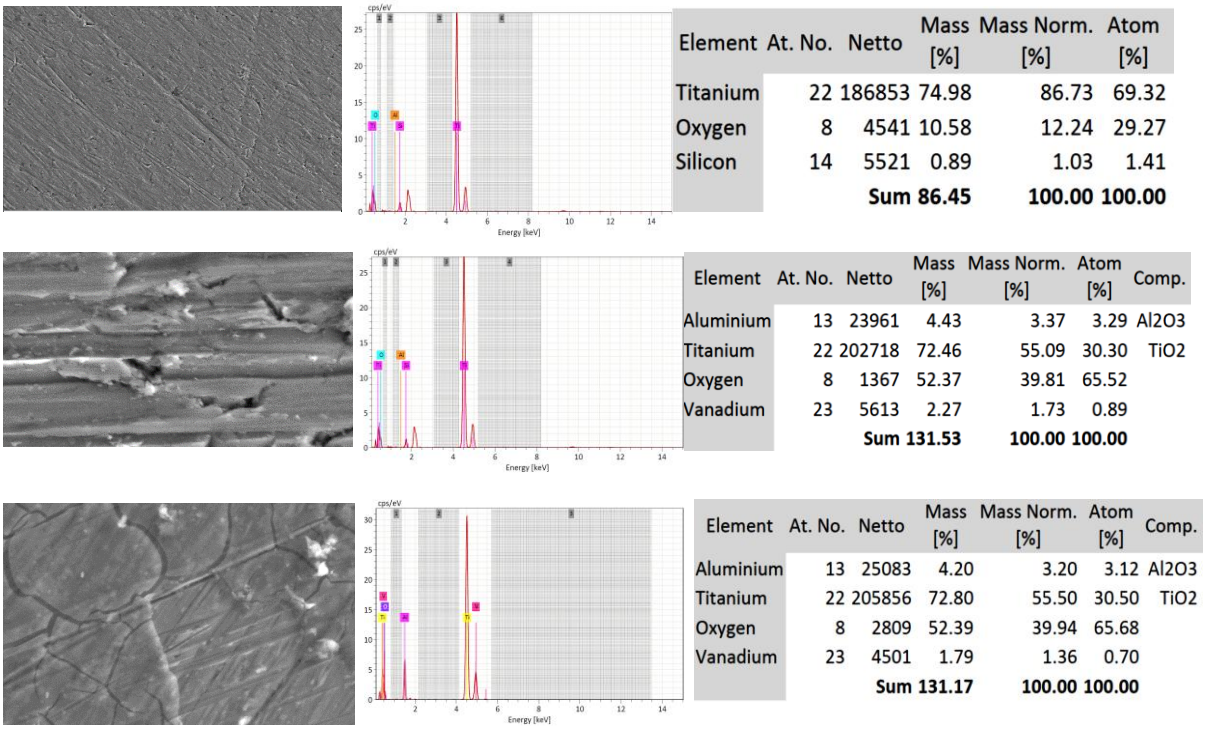

Element	At. No.	Netto	Mass [%]	Mass Norm. [%]	Atom [%]
Titanium	22	186853	74.98	86.73	69.32
Oxygen	8	4541	10.58	12.24	29.27
Silicon	14	5521	0.89	1.03	1.41
		Sum	**86.45**	**100.00**	**100.00**

Element	At. No.	Netto	Mass [%]	Mass Norm. [%]	Atom [%]	Comp.
Aluminium	13	23961	4.43	3.37	3.29	Al2O3
Titanium	22	202718	72.46	55.09	30.30	TiO2
Oxygen	8	1367	52.37	39.81	65.52	
Vanadium	23	5613	2.27	1.73	0.89	
		Sum	**131.53**	**100.00**	**100.00**	

Element	At. No.	Netto	Mass [%]	Mass Norm. [%]	Atom [%]	Comp.
Aluminium	13	25083	4.20	3.20	3.12	Al2O3
Titanium	22	205856	72.80	55.50	30.50	TiO2
Oxygen	8	2809	52.39	39.94	65.68	
Vanadium	23	4501	1.79	1.36	0.70	
		Sum	**131.17**	**100.00**	**100.00**	

Fig. 10: SEM images and EDX analysis after 120 h immersion in simulated inflammation solution of (a) pure Ti, (b) Ti-4Al-2V alloy (c) Ti-6Al-4V alloy at 37°C.

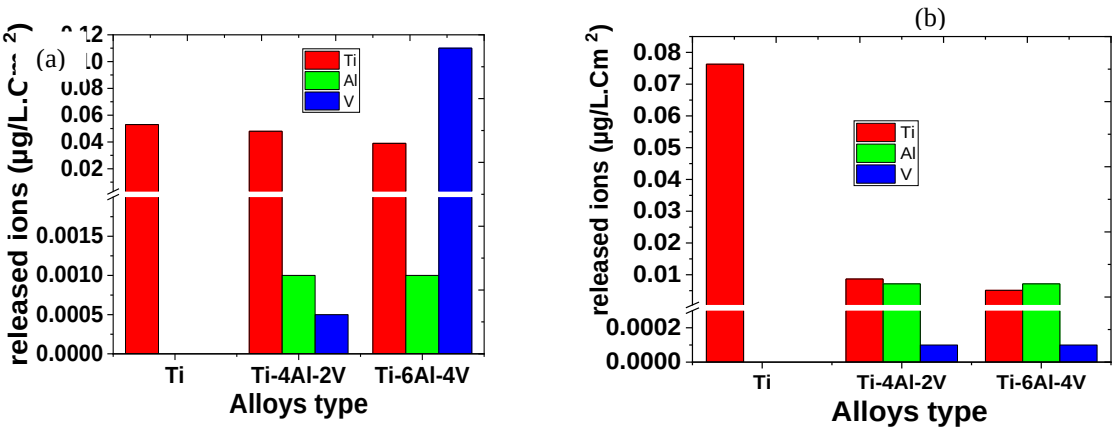

Fig. 11: Total concentration of Ti, Al, V release from Ti and its alloys after 120 h immersion of the electrode in (a) SBF/H_2O_2 and (b) SBF solutions at 37 °C.

References

[1] H.-F. Li, J.-Y. Huang, G.-C. Lin, P.-Y. Wang, *Rare Metals* **2021**, *40*, 3091-3106. 10.1007/s12598-021-01796-z

[2] S. Malik, V. Kumar, *Surface Review and Letters* **2021**, *30*, 2141007. 10.1142/S0218625X21410079

[3] F. J. O'Brien, *Materials Today* **2011**, *14*, 88-95. https://doi.org/10.1016/S1369-7021(11)70058-X

[4] H. Liu, M. Niinomi, M. Nakai, S. Obara, H. Fujii, *Materials Science and Engineering: A* **2017**, *704*, 10-17. https://doi.org/10.1016/j.msea.2017.07.078

[5] S. Sahoo, *International Journal of Nano and Biomaterials* **2014**, *5*, 228-235. 10.1504/IJNBM.2014.069811

[6] M. S. Baltatu, A. V. Sandu, M. Nabialek, P. Vizureanu, G. Ciobanu, in *Micromachines, Vol. 12*, **2021**. doi:10.3390/mi12121447

[7] X. Mao, A. Shi, R. Wang, J. Nie, G. Qin, D. Chen, E. Zhang, in *Metals, Vol. 12*, **2022**. doi:10.3390/met12071132

[8] H. Zhao, C. Zhao, W. Xie, D. Wu, B. Du, X. Zhang, M. Wen, R. Ma, R. Li, J. Jiao, C. Chang, X. Yan, L. Sheng, in *Materials, Vol. 16*, **2023**. doi:10.3390/ma16083250

[9] I. Vazirgiantzikis, I. *Investigation into the surface modification of Ti-6Al-4V to facilitate antimicrobial ionic silver integration for use in implantable orthopaedic devices.* Retrieved from http://hdl.handle.net/11427/33121 Available from University of Cape Town OpenUCT database.

[10] S. L. d. Assis, S. Wolynec, I. Costa, *Electrochimica Acta* **2006**, *51*, 1815-1819. https://doi.org/10.1016/j.electacta.2005.02.121

[11] J. Mouhyi, D. M. Dohan Ehrenfest, T. Albrektsson, *Clinical Implant Dentistry and Related Research* **2012**, *14*, 170-183. https://doi.org/10.1111/j.1708-8208.2009.00244.x

[12] A. Bordbar-Khiabani, M. Gasik, *Scientific Reports* **2023**, *13*, 2312. 10.1038/s41598-023-29553-5

[13] X. Han, J. Ma, A. Tian, Y. Wang, Y. Li, B. Dong, X. Tong, X. Ma, *Colloids and Surfaces B: Biointerfaces* **2023**, *227*, 113339. https://doi.org/10.1016/j.colsurfb.2023.113339

[14] L. Kunčická, R. Kocich, T. C. Lowe, *Progress in Materials Science* **2017**, *88*, 232-280. https://doi.org/10.1016/j.pmatsci.2017.04.002

[15] Y. L. Zhou, M. Niinomi, T. Akahori, H. Fukui, H. Toda, *Materials Science and Engineering: A* **2005**, *398*, 28-36. https://doi.org/10.1016/j.msea.2005.03.032

[16] M. Niinomi, M. Nakai, J. Hieda, *Acta Biomaterialia* **2012**, *8*, 3888-3903. https://doi.org/10.1016/j.actbio.2012.06.037

[17] P. Chui, R. Jing, F. Zhang, J. Li, T. Feng, *Journal of Alloys and Compounds* **2020**, *842*, 155693. https://doi.org/10.1016/j.jallcom.2020.155693

[18] L. Mohan, C. Anandan, V. K. W. Grips, *Applied Surface Science* **2012**, *258*, 6331-6340. https://doi.org/10.1016/j.apsusc.2012.03.032

[19] F. Cai, Q. Zhou, J. Chen, S. Zhang, *Corrosion Science* **2023**, *213*, 111002. https://doi.org/10.1016/j.corsci.2023.111002

[20] C. A. Escobar Claros, L. Contri Campanelli, A. Moreira Jorge, J.-C. Leprêtre, C. Bolfarini, V. Roche, *Corrosion Science* **2021**, *188*, 109544. https://doi.org/10.1016/j.corsci.2021.109544

[21] S. Gurel, M. B. Yagci, B. Bal, D. Canadinc, *Materials Chemistry and Physics* **2020**, *254*, 123377. https://doi.org/10.1016/j.matchemphys.2020.123377

[22] M. Nadimi, C. Dehghanian, *Ceramics International* **2021**, *47*, 33413-33425. https://doi.org/10.1016/j.ceramint.2021.08.248

[23] A. Sharma, M. C. Oh, J.-T. Kim, A. K. Srivastava, B. Ahn, *Journal of Alloys and Compounds* **2020**, *830*, 154620. https://doi.org/10.1016/j.jallcom.2020.154620

[24] C. Xin, N. Wang, Y. Chen, B. He, Q. Zhao, L. Chen, Y. Tang, B. Luo, Y. Zhao, X. Yang, *Materials & Design* **2022**, *215*, 110540. https://doi.org/10.1016/j.matdes.2022.110540

[25] R. Pani, R. R. Behera, S. Roy, in *Handbook of Research on Corrosion Sciences and Engineering* (Eds.: Y. El Kacimi, L. Guo), IGI Global, Hershey, PA, USA, **2023**, pp. 246-273.

[26] X. Zhang, L. Zhang, D. Zhang, L. Han, J. Bai, Z. Huang, C. Guo, F. Xue, P. K. Chu, C. Chu, *Materials Chemistry and Physics* **2023**, *304*, 127838. https://doi.org/10.1016/j.matchemphys.2023.127838

[27] H. Ahn, D. Lee, K.-M. Lee, K. Lee, D. Baek, S.-W. Park, *Surface and Coatings Technology* **2008**, *202*, 5784-5789. https://doi.org/10.1016/j.surfcoat.2008.06.074

[28] F. Contu, *Journal of Biomedical Materials Research Part B: Applied Biomaterials* **2012**, *100B*, 544-552. https://doi.org/10.1002/jbm.b.31984

[29] F. Contu, B. Elsener, H. Böhni, *Corrosion Science* **2004**, *46*, 2241-2254. https://doi.org/10.1016/j.corsci.2004.01.005

[30] S. Karimi, T. Nickchi, A. Alfantazi, *Corrosion Science* **2011**, *53*, 3262-3272. https://doi.org/10.1016/j.corsci.2011.06.009

[31] M. Koike, H. Fujii, *Journal of Oral Rehabilitation* **2001**, *28*, 540-548. https://doi.org/10.1046/j.1365-2842.2001.00690.x

[32] Y. Okazaki, E. Gotoh, *Biomaterials* **2005**, *26*, 11-21. https://doi.org/10.1016/j.biomaterials.2004.02.005

[33] N. Padilla, A. Bronson, *Journal of Biomedical Materials Research Part A* **2007**, *81A*, 531-543. https://doi.org/10.1002/jbm.a.31046

[34] J. Pan, D. Thierry, C. Leygraf, *Journal of Biomedical Materials Research* **1996**, *30*, 393-402. https://doi.org/10.1002/(SICI)1097-4636(199603)30:3<393::AID-JBM14>3.0.CO;2-L

[35] R. Strietzel, A. Hösch, H. Kalbfleisch, D. Buch, *Biomaterials* **1998**, *19*, 1495-1499. https://doi.org/10.1016/S0142-9612(98)00065-9

[36] R. L. Williams, S. A. Brown, K. Merritt, *Biomaterials* **1988**, *9*, 181-186. https://doi.org/10.1016/0142-9612(88)90119-6

[37] T. Okoko, *Journal of Genetic Engineering and Biotechnology* **2018**, *16*, 485-490. https://doi.org/10.1016/j.jgeb.2018.02.004

[38] H.-Y. Lin, J. D. Bumgardner, *Applied Surface Science* **2004**, *225*, 21-28. https://doi.org/10.1016/j.apsusc.2003.09.027

[39] J. M. Anderson, A. Rodriguez, D. T. Chang, *Seminars in Immunology* **2008**, *20*, 86-100. https://doi.org/10.1016/j.smim.2007.11.004

[40] B. M. Babior, R. S. Kipnes, J. T. Curnutte, *The Journal of clinical investigation*

1973, *52*, 741-744. https://www.jci.org/articles/view/107236

[41] E. Brooks, M. Tobias, K. Krautsak, M. Ehrensberger, *Journal of Biomedical Materials Research Part B: Applied Biomaterials* **2014**, *102*, 1445-1453. https://doi.org/10.1002/jbm.b.33123

[42] J. Pan, D. Thierry, C. Leygraf, *Electrochimica Acta* **1996**, *41*, 1143-1153. https://doi.org/10.1016/0013-4686(95)00465-3

[43] L. Dragus, L. Benea, N. Simionescu, A. Ravoiu, V. Neaga, *IOP Conference Series: Materials Science and Engineering* **2019**, *572*, 012005. 10.1088/1757-899X/572/1/012005

[44] C. Fonseca, M. A. Barbosa, *Corrosion Science* **2001**, *43*, 547-559. https://doi.org/10.1016/S0010-938X(00)00107-4

[45] F. L. Nie, S. G. Wang, Y. B. Wang, S. C. Wei, Y. F. Zheng, *Dental Materials* **2011**, *27*, 677-683. https://doi.org/10.1016/j.dental.2011.03.009

[46] W. A. Badawy, M. M. El-Rabiei, H. Nady, *Electrochimica Acta* **2014**, *120*, 39-45. https://doi.org/10.1016/j.electacta.2013.12.043

[47] R. G. Blundy, M. J. Pryor, *Corrosion Science* **1972**, *12*, 65-75. https://doi.org/10.1016/S0010-938X(72)90567-7

[48] K. M. Ismail, A. M. Fathi, W. A. Badawy, *Journal of Applied Electrochemistry* **2004**, *34*, 823-831. 10.1023/B:JACH.0000035612.66363.a3

[49] I. Milošev, M. Metikoš-Huković, *Electrochimica Acta* **1997**, *42*, 1537-1548. https://doi.org/10.1016/S0013-4686(96)00315-5

[50] G. Song, A. L. Bowles, D. H. StJohn, *Materials Science and Engineering: A* **2004**, *366*, 74-86. https://doi.org/10.1016/j.msea.2003.08.060

[51] N. A. Al-Mobarak, A. M. Al-Mayouf, A. A. Al-Swayih, *Materials Chemistry and Physics* **2006**, *99*, 333-340. https://doi.org/10.1016/j.matchemphys.2005.10.032

[52] J. Gilbert, Z. Bai, Chandrasekaran N, inventors; Syracuse University, assignee. Method for preparing biomedical surfaces. U S Patent No 0,022,650;2012.